



LASER INTERFEROMETER GRAVITATIONAL WAVE OBSERVATORY

*LIGO Laboratory / LIGO Scientific Collaboration*

LIGO-T040119-00-R

*ADVANCED LIGO*

06/01/04

---

Mach-Zehnder interferometer for  
Advanced-LIGO optical configurations  
to eliminate sidebands of sidebands

---

Osamu Miyakawa, Seiji kawamura, Bryan Barr, Stephen Vass

*Distribution of this draft:*  
LIGO Science Collaboration

**California Institute of Technology**

**LIGO Project - MS 18-34**

**Pasadena, CA 91125**

Phone (626) 395-2129

Fax (626) 304-9834

E-mail: [info@ligo.caltech.edu](mailto:info@ligo.caltech.edu)

**Massachusetts Institute of Technology**

**LIGO Project - NW17 - 161**

**Cambridge, MA 01239**

Phone (617) 253-4824

Fax (617) 253-7014

E-mail: [info@ligo.mit.edu](mailto:info@ligo.mit.edu)

**LIGO Hanford Observatory**

**P.O. Box 1970**

**Mail Stop S9-02**

**Richland, WA 99352**

Phone (509) 372-8106

Fax (509) 372-8137

**LIGO Livingston Observatory**

**P.O. Box 940**

**Livingston, LA 70754**

Phone (225) 686-3100

Fax (225) 686-7189

<http://www.ligo.caltech.edu/>

**Abstract**

The sidebands of sidebands produced by two EOMs in series will be a serious problem in the optical configuration for Advanced-LIGO. This paper describes the performance when a Mach-Zehnder interferometer having two EOMs in parallel is installed on the PSL of the 40m prototype to avoid the sidebands of sidebands.

## 1 Introduction

Two modulations using two EOMs are used in the optical configuration of Advanced-LIGO[1, 2, 3] (AdvLIGO) to extract control signals of the central part (including Michelson, power recycling cavity and signal extraction cavity). The signals of the central part are extracted from the beats between two sidebands (not the beats between carrier and sidebands), therefore this method has little influence from the carrier on control of the central part and helps to diagonalize the signal matrix. Caltech's 40m[4] is a prototype interferometer for the optical configuration of AdvLIGO and has been prepared to investigate a lock acquisition scheme and noise performance. However, in the experiment at the 40m, we found that two EOMs in series produce sidebands impressed on sidebands and cause undesired beating between carrier and sidebands of sidebands[5, 6]. This effect cancels an otherwise expected DC offset in the signals at any non-resonant point, and degrades the diagonalization of the signal matrix as shown in Tables 1,2. A cross coupling of greater than unity in the normalized matrix is not desirable. At first glance, offset cancellation sounds desirable, but the offset can be used as an indicator for adjusting demodulation phase, so it cannot be said that no offset is better.

We expect that the introduction of a Mach-Zehnder interferometer into the PSL of the 40m is the best method (at least from a practical stand point) of eliminating these sidebands of sidebands.

Table 1: Signal matrix with the ideal cavity length.

Port	Dem. freq.	Dem. phase	$L_+$	$L_-$	$l_+$	$l_-$	$l_s$
SP	$f_1$	10	1	-3.8E-9	-1.2E-3	-1.3E-6	-2.3E-6
AP	$f_2$	271	-4.8E-9	1	-1.2E-8	-1.3E-3	-1.7E-8
SP	$f_1 \times f_2$	189,32	-1.7E-3	-3.0E-4	1	-3.2E-2	-1.0E-1
AP	$f_1 \times f_2$	4,81	-6.2E-4	1.5E-3	7.5E-3	1	7.1E-2
PO	$f_1 \times f_2$	164,12	3.6E-3	2.7E-3	4.6E-1	-2.3E-2	1

Table 2: Signal matrix with sidebands of sidebands.

Port	Dem. freq.	Dem. phase	$L_+$	$L_-$	$l_+$	$l_-$	$l_s$
SP	$f_1$	10	1	-1.4E-8	-1.2E-3	-1.4E-6	-6.2E-6
AP	$f_2$	271	1.2E-7	1	1.4E-5	1.3E-3	6.5E-6
SP	$f_1 \times f_2$	184,30	7.4	-3.4E-4	1	-3.3E-2	-1.1E-1
AP	$f_1 \times f_2$	4,73	-5.7E-4	32	7.1E-1	1	7.1E-2
PO	$f_1 \times f_2$	161,4	3.3	1.7	1.9E-1	-3.5E-2	1

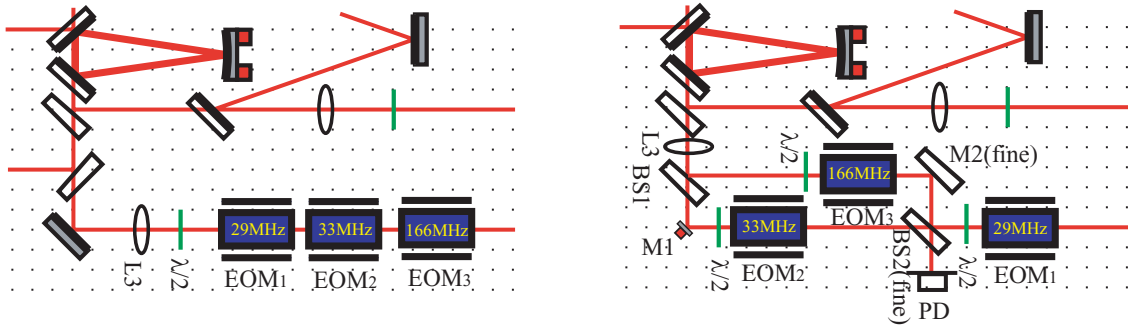


Figure 1: Present setting of EOMs downstream of PMC (left) and a with new Mach-Zehnder interferometer (right).

## 2 Mach-Zehnder interferometer

Figure 1 shows an optical configuration for the Mach-Zehnder interferometer. Light from the pre-mode cleaner (PMC) is divided by the first beams splitter ( $BS_1$ ) at a ratio of 50:50. Each beam then enters an EOM and is modulated at 33 MHz or 166 MHz. The beams are then recombined by another beam splitter ( $BS_2$ ) and the light is divided into two ports. The Mach-Zehnder interferometer will be controlled such that all the light will exist the bright port (BP) and go to the interferometer with other port remaining dark (DP).

In a Mach-Zehnder interferometer, the sidebands of sidebands do not exist from the beginning because the EOMs are placed in parallel and each sideband is generated independently. However, it creates the following complications;

- To control one more degree of freedom
- Sideband power reduced by factor of 4
- Making both arms have equal length
- Mode matching
- Excess noise (intensity noise, frequency noise)

It is necessary to control one more mirror. The reason for this is that microscopic differences of arm length generate amplitude fluctuations when the light is recombined at the beam splitter.

The sidebands generated by two EOMs have 1/4 the power compared with the series modulations. This is because the sidebands are generated from a half carrier (divided by  $BS_1$ ), and they get halved again when compared with the summed carrier when the light is recombined at  $BS_2$ : unlike the carrier, no construction interference occurs for the sidebands at the bright port, and thus half the power in each set of sidebands is lost through the  $BS_2$ .

The length of both arms must be the same as much as possible. Otherwise, the effect of the lens which comes afterwards will be different for each arm and the mode matching ratio will be different. However, this is the mode matching to the mode cleaner (MC), and after light passes the

mode cleaner, this mismatch will not be a problem for the interferometer because it is suppressed by a factor of  $1/\text{finesse}$  of the MC.

Because it is necessary to move the position of the lens which focuses on the EOMs as shown in Fig. 1, it will be necessary to adjust the mode matching.

The Mach-Zehnder interferometer has the potential to introduce more noise. We consider frequency noise and intensity noise here in Section 4.

### 3 Control using internal modulation

Here, internal modulation is assumed to be the control method for the Mach-Zehnder interferometer, therefore only one EOM will be placed in the transmitted port of the BS<sub>1</sub>.

The laser carrier  $E$  is described as

$$E = E_i e^{-i\omega_0 t}, \quad (1)$$

where  $\omega_0$  is an angular frequency of the laser, and  $E_i$  is the amplitude of the incident laser into the Mach-Zehnder interferometer. The laser is divided by the first beam splitter which has  $1/\sqrt{2}$  amplitude reflectivity and  $1/\sqrt{2}$  amplitude transmissivity. One beam is phase modulated by the EOM, therefore the amplitude of the carrier and the first order sidebands before the second beam splitter can be written as

$$\frac{E_t}{E_i} = \frac{1}{\sqrt{2}} J_0(m) e^{-i\phi_t} + i \frac{1}{\sqrt{2}} J_1(m) e^{-i(\phi_t + \phi_m)} + i \frac{1}{\sqrt{2}} J_1(m) e^{-i(\phi_t - \phi_m)} \quad (2)$$

$$\frac{E_r}{E_i} = \frac{1}{\sqrt{2}} e^{-i\phi_r}, \quad (3)$$

where  $E_t$  is the amplitude at the transmitted port of BS<sub>1</sub> and  $E_r$  is the amplitude at the reflected port of BS<sub>1</sub>.  $J_0$  and  $J_1$  are the 0th/1st order Bessel function and  $m$  is a modulation index.  $\phi_t$  is a phase change from the transmitted port of BS<sub>1</sub> to BS<sub>2</sub> and  $\phi_r$  is a phase change from the reflected port of BS<sub>1</sub> to BS<sub>2</sub>.  $\phi_m$  is additional phase change of sideband compared with the carrier from the EOM to the BS<sub>2</sub> shown as

$$\phi_m = \frac{l_t \omega_m}{c} \quad (4)$$

where  $l_t$  is length from the EOM to BS<sub>2</sub>,  $\omega_m$  is the angular frequency of the modulation and  $c$  is the speed of light.

The light at the DP can be written

$$\frac{E_0}{E_i} = \left( \frac{1}{2} e^{-i\phi_r} - \frac{1}{2} J_0(m) e^{-i\phi_t} \right) \quad (5)$$

$$\frac{E_1}{E_i} = -\frac{1}{2} i J_1(m) e^{-i(\phi_r + \phi_m)} \quad (6)$$

$$\frac{E_{-1}}{E_i} = -\frac{1}{2} i J_1(m) e^{-i(\phi_r - \phi_m)}, \quad (7)$$

where  $E_0$  is the amplitude of the carrier in the DP and  $E_{\pm 1}$  is the amplitude of the upper/lower sideband in the DP.

An error signal  $V_{\text{error}}$  can be extracted when the light is photo detected and demodulated as

$$V_{\text{error}} = -\text{Im}(E_0^* E_1 - E_0 E_{-1}^*) \quad (8)$$

which simplifies to

$$V_{\text{error}} = \frac{1}{2} \text{Im}(e^{-i\phi_m}) J_1(m) \sin(\phi_-) E_i \quad (9)$$

where  $\phi_- = \phi_r - \phi_t$  is a differential mode of each arm. Here,  $\text{Im}(e^{-i\phi_m})$  is an undetermined factor and it can be maximized by the demodulation phase.

Fig. 2 shows the error signal at the DP in Eq. 9. The Mach-Zehnder interferometer can be controlled by feeding back this error signal to the mirror so that all of the carrier transmits to the interferometer side (bright port).

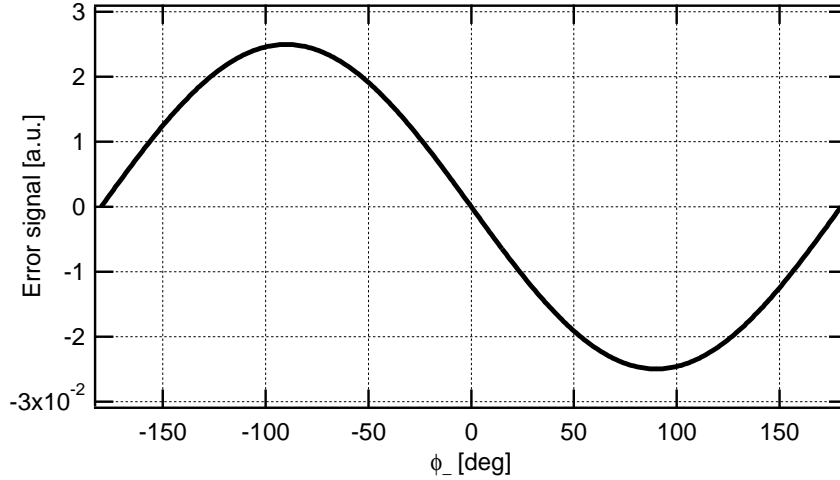


Figure 2: Error signal of Mach-Zehnder interferometer.

## 4 Excess noise caused by Mach-zehnder interferometer

### 4.1 Frequency noise

It is understood that each steering mirror used on the PSL table usually generates frequency noise around 800 Hz caused by a Doppler shift or beam jitter (See Fig. 3). Frequency noise in the mirrors upstream of the PMC are negligible because they are suppressed by the PMC but the mirrors downstream of the PMC will be a problem. Three new mirrors will be introduced by the Mach-Zehnder interferometer as shown Fig. 1.

It is assumed that similar mirrors and similar mirror mounts will be used, and each mirror has noise  $n$ . The total noise with new mirrors will then be

$$\sqrt{\frac{6n^2}{3n^2}} = \sqrt{2} \quad (10)$$

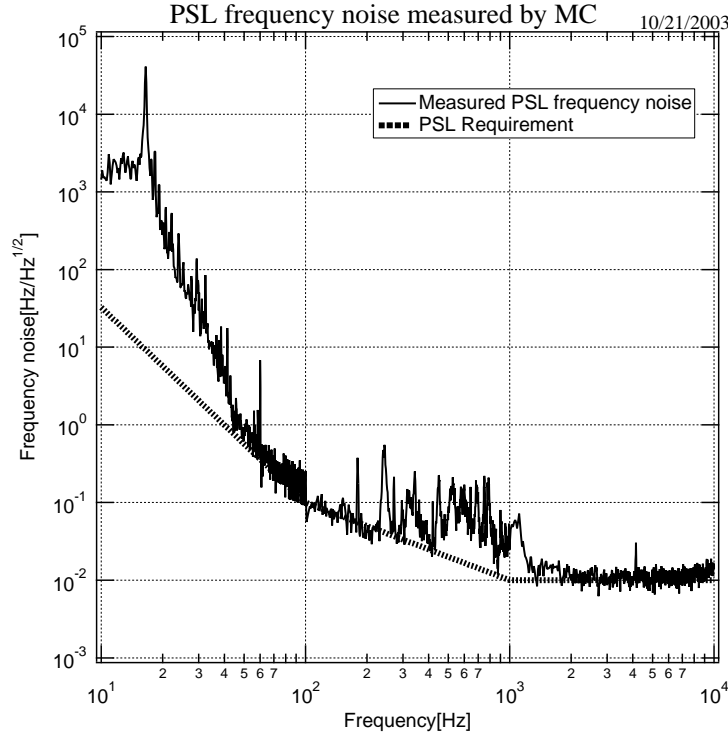


Figure 3: PSL frequency noise measured by MC.

times larger than before. Four ports are necessary for BS2, so at least one mirror mount will be different from the others. It is possible that the frequency noise may increase due to this difference. It would be possible to put the Mach-Zehnder interferometer in the FSS loop if the frequency noise does not meet this specification.

## 4.2 Intensity noise

Figure 4 shows a relative intensity noise downstream of the PMC and an expected relative intensity noise which will be added by introducing the Mach-Zehnder interferometer. This expected noise is comes from two sources: one is the differential motion of each length around 1 Hz, and another one is resonant peaks of the mirrors and the mounts around 1 kHz.

It is known that a fixed mirror on the optical table is typically shaking with an amplitude of  $\lambda/10$  around 1 Hz from the table top Michelson interferometer experiment. This is divided by the wave length  $\lambda$  to convert into a fluctuation of phase. Around the operating point of the Mach-Zehnder interferometer, the fluctuation of the phase can be converted to the relative intensity noise as a second order effect. In this case, it becomes  $1/100$  at 1 Hz. The existing relative intensity noise of the laser is approximately  $10^{-4}/\sqrt{\text{Hz}}$  around 1 Hz, therefore, the gain of  $10^2$  is needed around 1 Hz to suppress the intensity noise caused by the Mach-Zehnder interferometer.

It is also known that the fixed steering mirror which will be used on the Mach-Zehnder interferometer has a resonant peak around 800 Hz. We evaluate the intensity noise the due to this

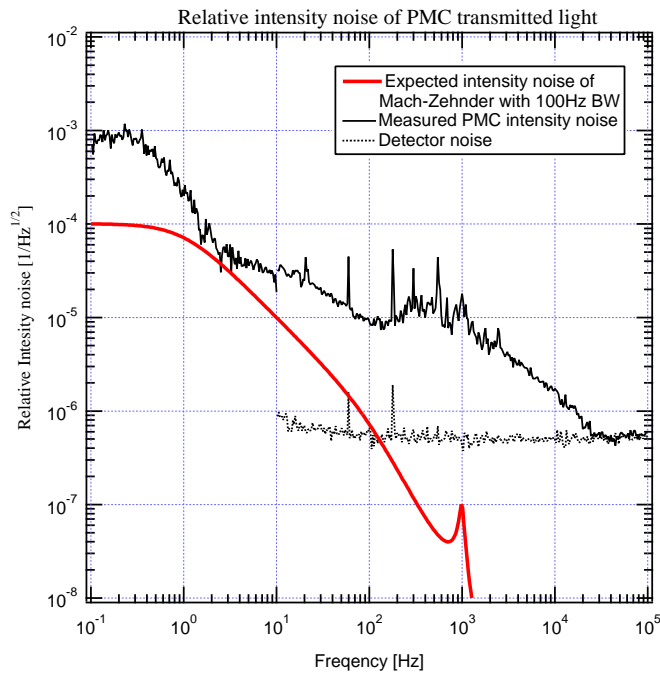


Figure 4: Relative intensity noise of PMC and expecting relative intensity noise of Mach-Zehnder interferometer.

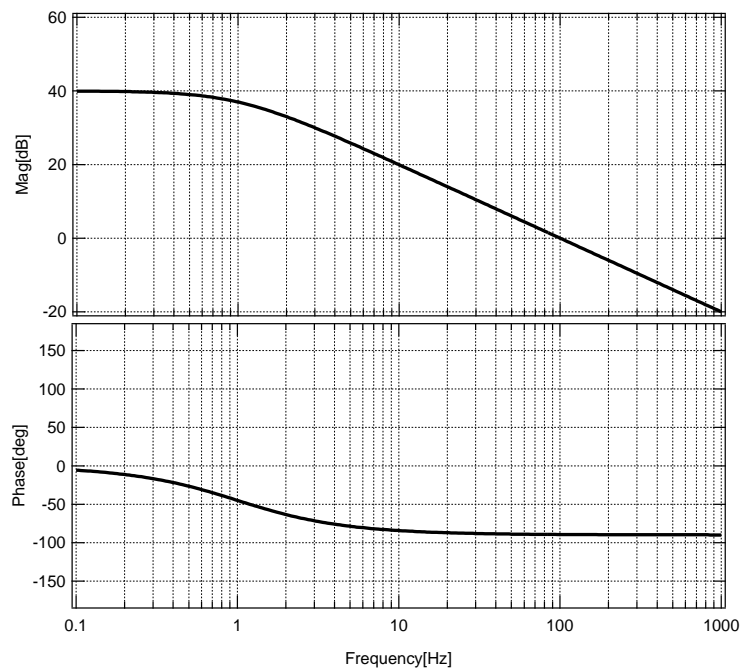


Figure 5: Open loop transfer function of Mach-Zehnder interferometer on the PSL of 40m.



resonances using the PSL frequency noise measured by the MC as shown in Fig. 3. Many peaks which have  $\delta f \approx 3 \times 10^{-1} \text{ Hz}/\sqrt{\text{Hz}}$  of the frequency noise can be seen from 200 Hz to 1 kHz. To convert this frequency noise into phase noise  $\delta\phi$ , the relationship of

$$\frac{\delta f}{f} = \frac{\delta\phi}{2\pi} \quad (11)$$

is used and here we assume that  $f = 1 \text{ kHz}$ , therefore the phase fluctuation of  $\delta\phi/2\pi$  will be  $3 \times 10^{-4} \text{ Hz}/\sqrt{\text{Hz}}$ . This can be converted to the relative intensity noise as a second order effect around the operating point. The relative intensity noise will be  $1 \times 10^{-7} \text{ Hz}/\sqrt{\text{Hz}}$ . This is much smaller than the existing intensity noise even if there is no control. If quality factor (Q factor) of the mirror resonance is assumed to be 10, it can be assumed that the noise floor will drop from 1 to 1 kHz with  $f^{-2}$ .

We assume that -1 order low-pass filter is used as a feedback filter with a pole at 1 Hz. It is preferable to put this low-pass filter in the final stage after the PZT driver to avoid the loss of the dynamic range and to make noise smaller. An expected open loop transfer function is shown in Fig. 5. The expected intensity noise by the Mach-Zehnder interferometer will be negligible with this gain as shown in Fig. 4. Note that only one peak is shown in Fig. 4, but it is expected that there will actually be as many peaks as there are steering mirrors.

## 5 Requirements

- The dynamic range of PZT: the relative temperature fluctuation of the arms is assumed to be 0.1 K or less. Total daily temperature change is 1.5 K on the PSL table at most. The coefficient of thermal expansion of the PSL optical table is  $1 \times 10^{-5} \text{ m/K}$ . The length change in each optical path due to temperature fluctuation will be  $10^{-6} \text{ m}$  If the distance between separating the arms is 10 cm. Therefore, it is necessary to have at least  $1\mu\text{m}$  of dynamic range.
- Mirror mass : as low as possible
- Resonant frequency: greater than 10 kHz
- Gain:  $1 \times 10^2$  at 1 Hz
- Band width (unity gain frequency): 100 Hz
- PZT driver: greater than 100 V DC, and greater than 10 kHz in band width

## 6 Specifications

- Beam splitter ( $\text{BS}_1$ ): CVI BS-1064-50-1025-45P, for 1064 nm,  $45^\circ$  incident angle for P polarization
- Control mirror ( $\text{M}_1$ ): CVI Y1-0316-45P,  $\phi 0.3''$ ,  $t 0.16''$  for 1064 nm,  $45^\circ$  incident angle for P polarization
- PZT: Kenetic Ceramics. Inc. D1CM10, 0.06 $\mu\text{F}$ , Res. Freq. 125 kHz,  $10\mu\text{m}$  at 1000 V

- PZT driver: standard LIGO PZT driver (same as PMC's PZT driver)
- Half wave plate: CVI QWPO-1064-06-2-R10
- EOM<sub>1</sub>: New Focus 4003, 33MHz resonant
- EOM<sub>2</sub>: New Focus 4003, 166MHz resonant
- Steering mirror (M<sub>2</sub>): CVI Y1-1025-45S for 1064 nm, 45° incident angle for S polarization
- Mount (for BS<sub>1</sub>, M<sub>1</sub> and M<sub>2</sub>): Newport U100-AC
- Beam splitter (BS<sub>2</sub>): CVI BS-1064-50-1025-45S, for 1064 nm, 45° incident angle for S polarization
- Mount (for BS<sub>2</sub>): Newport SK45
- Micrometer (for M<sub>2</sub>,BS<sub>2</sub>): Newport DM17-25, 0.1 μm resolution for fine alignment
- Photo detector: standard LIGO PD, 33MHz peak
- Demodulator: standard LIGO I&Q demod., 33MHz
- Filter: Stanford SR560, variable gain and variable frequency of low, high or band-pass filter

## 7 Summary

We discussed use of two EOMs in parallel using a Mach-Zehnder interferometer to eliminate sidebands of sidebands. The effect on the sideband is a power reduction by a factor of 4 compared with the usual seires modulation. The intensity noise can be negligible with enough gain. The frequency noise is not a serious problem if mirrors and mounts similar to those already in use on the PSL are used.

There is no serious problem in the use of the Mach-Zehnder interferometer to eliminate the sidebands of sidebands.

## References

- [1] E. Gustafson, D. Shoemaker, K. Strain, and R. Weiss. LSC white paper on detector research and development. *LIGO Document Number*, M990288-A-M, 1999.
- [2] LIGO II conceptual project book. *LIGO Document Number*, M990080-00-D, 1999.
- [3] Guido Mueller, David Reitze, Haisheng Rong, David Tanner, Sany Yoshida, and Jordan Camp. Reference design document for the Advanced LIGO Input Optics. *LIGO Document Number*, T010002-00-D, 2000.
- [4] A. Weinstein. Advanced LIGO optical configuration and prototyping effort. *Class. Quantum, Grav.*, 19:1575, 2002.

- [5] Osamu Miyakawa, Seiji Kawamura, Benjamin Abbott, Rolf Bork, Peter Fritschel, Lisa Goggin, Jay Heefner, Alexander Ivanov, Fumiko Kawazoe, Conor Mow-Lowry, Alexei Ourjoumtsev, Sihori Sakata, Michael Smith, Kenneth Strain, Rober Taylor, Dennis Ugolini, Stephen Vass, Robert Ward, , and Alan Weinstein. Sensing and control of the advanced ligo optical configuration. *LIGO Document Number*, P040017-00-R, 2004.
- [6] Bryan Barr, Osamu Miyakawa, and Seiji Kawamura. Sidebands of sidebands in the 40m system. *LIGO Document Number*, T040117-00-R, 2004.